Exploration of the Geological Formations of the Luquillo Mountain Range of North Eastern Puerto Rico using X-ray Florescence

Cindy Nawal

This study would have not been possible without the support and help of The Luquillo Critical Zone Observatory (LCZO). Professor Fred Scatena, Dr David R Vann and Jamie Horvath Special thanks to Professor Robert Giegengack, Alonso Ramírez, – Scientific director El Verde field station Puerto Rico and all the staff at the El Verde Field Station and the travel support provided by the LCZO.

Exploration of the Geological Formations of the Luquillo Mountain Range of North Eastern Puerto Rico using X-ray Florescence

Cindy Shanta Nawal

ABSTRACT

X-ray Florescence (XRF) is a widely used non-destructive method that measures the elemental composition of materials. This technology was applied to investigate the rocks and sediments in the Luquillo Mountains / El Yunque region of Puerto Rico. Initial testing of wet and dry sediments revealed that the machine records higher elemental concentrations in dry compared to wet sediments as it seems that the water molecules interfere with the X-ray beam on wet samples. The XRF method on dried samples produced reliable results and allowed for the chemical separation of the five basic bedrock types found in the Luquillo Mountains. Of the volcanoclastic the Fajardo Formation can be distinguished from the others by its concentration of Barium (Ba) and Rubidium (Rb). The Unnamed formation was distinguished by Copper (Cu) and the Hato Puerto Formation was distinguished by Nickel (Ni) and Strontium (Sr). The Rio Blanco granodiorite is the youngest rock type of the region and was the only formation whose elemental chemistry was not distinguishable from the others apparently because it was formed directly from the basic magma that also formed the Luquillo Mountains volcanic rocks. Recent studies have found high levels of Mercury (Hg) in Luquillo stream water. Knowing that the Luquillo region was heavily mined for Gold (Ag) and Silver (Au), the Hg used in historic mining is a possible source of the elevated Hg values. The XRF analysis indicated small quantities of Hg in some rocks but no Hg was found in the sediments and soils surrounding the historic mining sites. Therefore if Hg had been used in historic mining operations it is no longer apparent in the sediments and has presumably been removed by erosion of the site.

INTRODUCTION

The Luquillo Mountains are located in the northern eastern half of the island of Puerto Rico and range in elevation from 100-1075m above sea level. Also known as the El Yunque region, it once represented the most prosperous gold mining region on the island *(Cardona, 1984).* Mining began in 1508 but came to a halt in the 1880's due to the lack of a work force and late payment of mine claiming fees. Recurring hurricanes and landslides also hampered the mining activity in the region. *(Cardona, 1984)*

In 2007, a study was carried out by the United States Geologic Services (USGS) that compared Hg dynamics in five (5) diverse forested headwater catchments to determine Hg's fate and bioavailability *(Shanley et al 2008).* The research was focused in the forested upland headwaters since Hg deposition is enhanced at greater elevations and because the forest canopy can harbour a large pool of Hg. Of the 5 study watersheds the Luquillo watershed had the highest concentration of Total Mercury (THg) and Methyl Mercury (MeHg) and had a high flow concentration of 112ng L^{-1}.

PURPOSE OF STUDY

This study had two objectives. First to examine how well a hand held X ray fluoresce machine can differentiate the chemistry of the various rock types in the Luquillo Mountains. The second objective was to examine the concentration of Hg ions that are found within the sediments near historic mine sites to determine if former mining is responsible for the relatively high concentrations of Hg in Luquillo stream water (*Shanley et al 2008*).

The study was done by analysing sediments and rocks in areas near and away from former gold mines within the El Yunque region.

BACKGROUND

The Luquillo Mountains are covered by humid tropical rain forest. The region has undergone dramatic environmental change due to the combination of reforestation of former agricultural land and local urbanization. External driven changes such as variation in weather, extreme rainfall events, natural and human induced climate change have all been contributors of environmental change at a local level. *(Murphy et al 2009)*

Four (4) main watersheds can be found within the upper portion of the Luquillo Mountains. They include the Rio Icacos, the Rio Fajardo, the Rio Espirtu Santo and the Rio Mameyes (*Webb; Gomez; 1998*).The Rico Icacos drains the coarse grained granitic rocks and the Rio Mameyes the volcanicastics rocks and sediments. The catchment areas of these watersheds vary with the underlying bedrock. Mature rainforest covers the Rio Icacos and Rio Mameyes catchments.

PHYSIOGRAPHY

Puerto Rico is an island located in the Greater Antilles and is approximately nine thousand (9000) km^2 in area. The island has undergone transformation from pre European conditions of undisturbed forest to intensive agriculture in the nineteenth (19^{th}) and twentieth (20^{th}) century and an industrial revolution in the late 1950's. The industrialization has lead to over half of the land cover of the island being totally deforested *(Brandeis et al 2007).*

Puerto Rico is mountainous with central highland areas surrounded by flat lying coastal plains and alluvial valleys. *(Murphy et al 2009).* The Mameyes and Icacos watersheds drain the Luquillo Mountains. *(Ramos, Gines 1999)*

CLIMATE, EROSIONAL PROCESSES, VEGETATION AND LAND USE

Puerto Rico experiences a humid tropical climate and ranges in the daily temperature due to the assuaging effect of the ocean. *(Murphy et al 2009)* The topography of the island leads to variations in the wind speed, temperature, and rainfall. Generally the rainfall is greatest in the eastern mountains where the study site is

located and diminishes as you move westward rendering the southwest of the island in relatively arid. *(Murphy et al 2009).*

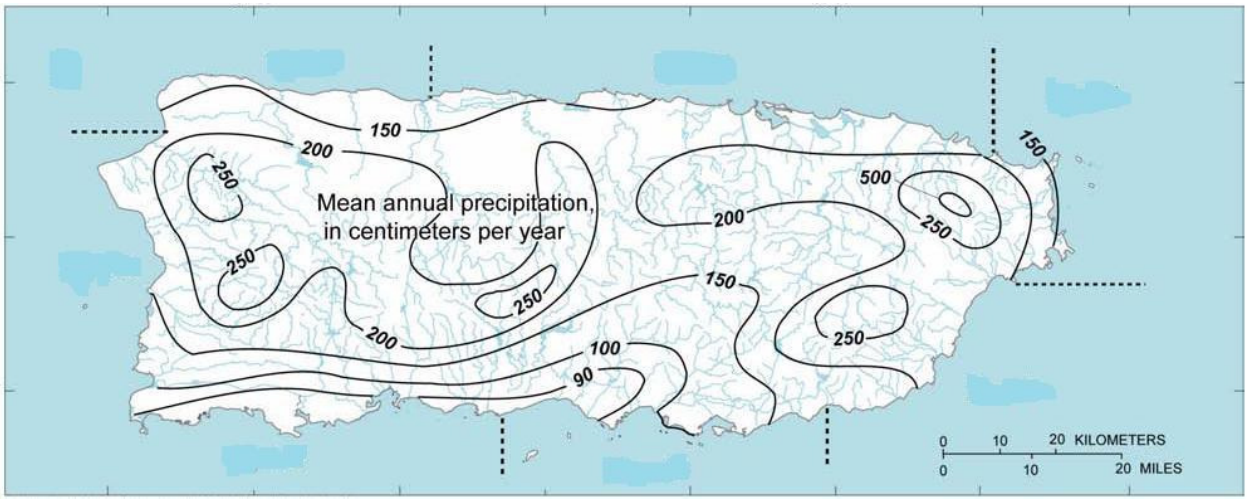

Figure 1.1 Showing the rainfall contours for the island of Puerto Rico (source: Warne, Andrew G; Webb, Richard M.T, Larsen Matthew C: Water***, Sediment, and Nutrient Discharge Characteristics of Rivers in Puerto Rico, and their Potential Influence***

Puerto Rico has a substantial portion of fluvial sediment that is transported from the mountains to the coast via hurricanes and large storms *(Warne et al 2005).* The storms that bring intense and prolonged rainfall are the leading cause of landslides on the island.

The clearing of the forest for agriculture that began in the 1800's is thought to have accelerated the rates of the rainfall triggered landslide events. *(Larsen, Stallard 2001).* During the period of extreme agricultural activity (1800-1950's) land clearance and agricultural activity have said to have increased the surface runoff by about fifty (50%) percent (*Clark, Wilcock 2001).*

REGIONAL GEOLOGY

Puerto Rico along with the northern Virgin Islands and St Croix represent the eastern edge of the Greater Antilles island arc. Arc volcanism in this region is associated with subduction in the north that began in the Cretaceous and continued till the Eocene *(Donovan, Jackson 1994).* Cessation of arc volcanism was accompanied by orogenesis that included folding, faulting and local uplift. This termination is thought to have been related to the collision of western Cuba with the Bahama Bank. From the Oligocene to the Holocene the

region surrounding the mountains was covered in limestone and sediments derived from weathering of the island arc. The Luquillo watersheds are underlained by marine deposited volcanoclastics with granitic intrusions.

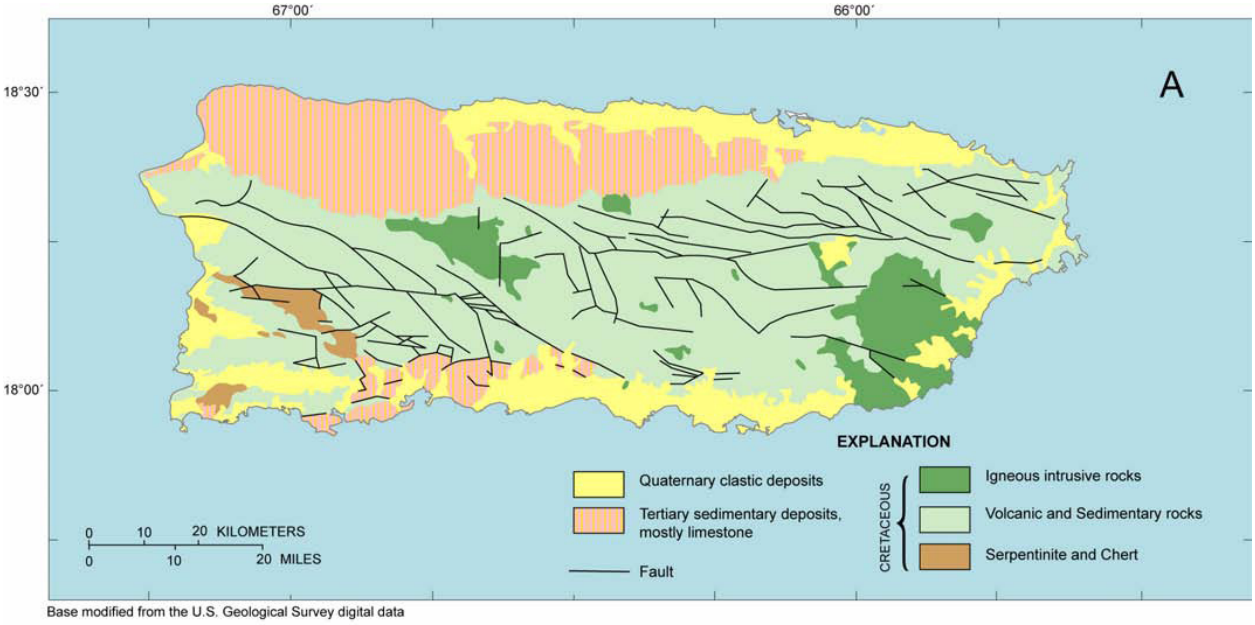

Fig 1.2 showing the generalised geology of Puerto Rico source: Warne, Andrew G; Webb, Richard M.T, Larsen Matthew C: Water***, Sediment, and Nutrient Discharge Characteristics of Rivers in Puerto Rico, and their Potential Influence***

The Luquillo Mountain watershed is underlained largely by marine deposited volcanoclastic rocks and granitic intrusions. Volcanoclastic rocks are formed as sediments that originated by volcanic process and were deposited in shallow marine environments *(Gillespie, Styles 1999).*Large scale folding and faulting has caused deformation of the strata and have resulted in westerly dips of strata that is increasingly younger as one moves westward *(Murphy et al 2009).*

Mameyes Watershed Geology

The Mameyes watershed is underlained by Cretaceous aged marine deposited volcanoclastic rock. The Fajardo, Tabonuco and Hato Puerco Formations underlie the Mameyes watershed where as the Rio Espirtu Santo watershed is almost entirely underlained by the Lomas Formations.

The Fajardo Formation is the oldest of the formations and ranges in age from 100-105 Mya and consists of thick bedded tuff breccias with large clasts of andesite. The Tabonuco Formation overlies the Fajardo Formation and consists of mudstone, volcanic sandstones, and sandstones that are less thickly bedded than the Fajardo Formation *(Murphy et al 2009).*The volcanic siltstones are moderately to well sorted, grey in colour and contain angular grains of plagioclase, clinopyroxene and quartz grains.

The Hato Puerco Formation overlies the Tabonuco and ranges in age from 90-97 Mya. The formation consists mostly of volcanic sandstone with grains of plagioclase, and hornblende *(Murphy et al 2009).* Calcareous mudstone and porphyritic lava are also present. The Lomas Formation found in the southern part of the Rio Espirtu Santo watershed consists of poorly sorted volcanic breccia and sandstone. The stratum also contains pumice and vesicular lava fragments and grains of plagioclase and clinopyroxene. The Lomas Formation does not have a depositional contact with the rest of the formations and occurs in fault blocks.

The Rio Blanco granodiorite stock intrudes and consequently metamorphosed the Fajardo, Tabonuco and Hato Puerco Formations. The resulting 2-4 km wide metamorphic contact zone acts as the watershed divide between the Mameyes and Icacos watershed. The metamorphosed rocks contain hornblende, garnet, epidote, chlorite, gold, copper, silver and iron sulphides veins. The weathering of the metamorphosed rocks is thought to have developed the gold deposits *(Cardona 1984).* Copper and gold bearing deposits were first worked by the Spaniards in the early 1500's.

Icacos watershed Geology

The Icacos watershed is underlained by Upper Cretaceous granitic rocks of the Rio Blanco Stock .The intrusion of the Rio Blanco Stock into the surrounding volcanoclastic rock is said to have occurred during the Eocene and represents the last phase of volcanism in the region. *(Murphy et al 2009)*

ECONOMIC GEOLOGY AND MINING HISTORY

While the main economic resources derived from the Luquillo Mountains are now water and recreation, historically the Luquillo Mountains were an important mining district *(Scatena 1989).*The copper mineral chalcopyrite has been found in veinlets along the metamorphosed zones of the Rio Blanco stock. Studies done in the La Mina region showed a peak concentration of 0.4 ppm of gold *(Sieders 1971)*. Further investigation yielded an extensive mineralized zone of chalcopyrite on the contact between the volcanoclastics of the Rio Blanco Stock on the Rio de La Mina. Sulphur, iron and mercury found from the region were featured at the 1882 Exposition Fair at Ponce. *(Sieders 1971)*Gold still occurs along nearly every brook and stream of the Luquillo Mountains *(Sieders 1971).*

MINING HISTORY

The mining of deposits in Puerto Rico occurred during the early colonization and the process was initiated by Juan Ponce de Leon in 1508 *(Cardona, 1984).* During the first 30 years the extraction has been calculated at 1,200,000 ounces of gold. The principal type of operation was placer mining along the most prominent rivers. Mining operations declined after 1529 when the colonists began substituting agriculture for gold mining. By 1882 placer mining on the island provided an estimated 2,000 to 3,000 Spanish pesos annually.

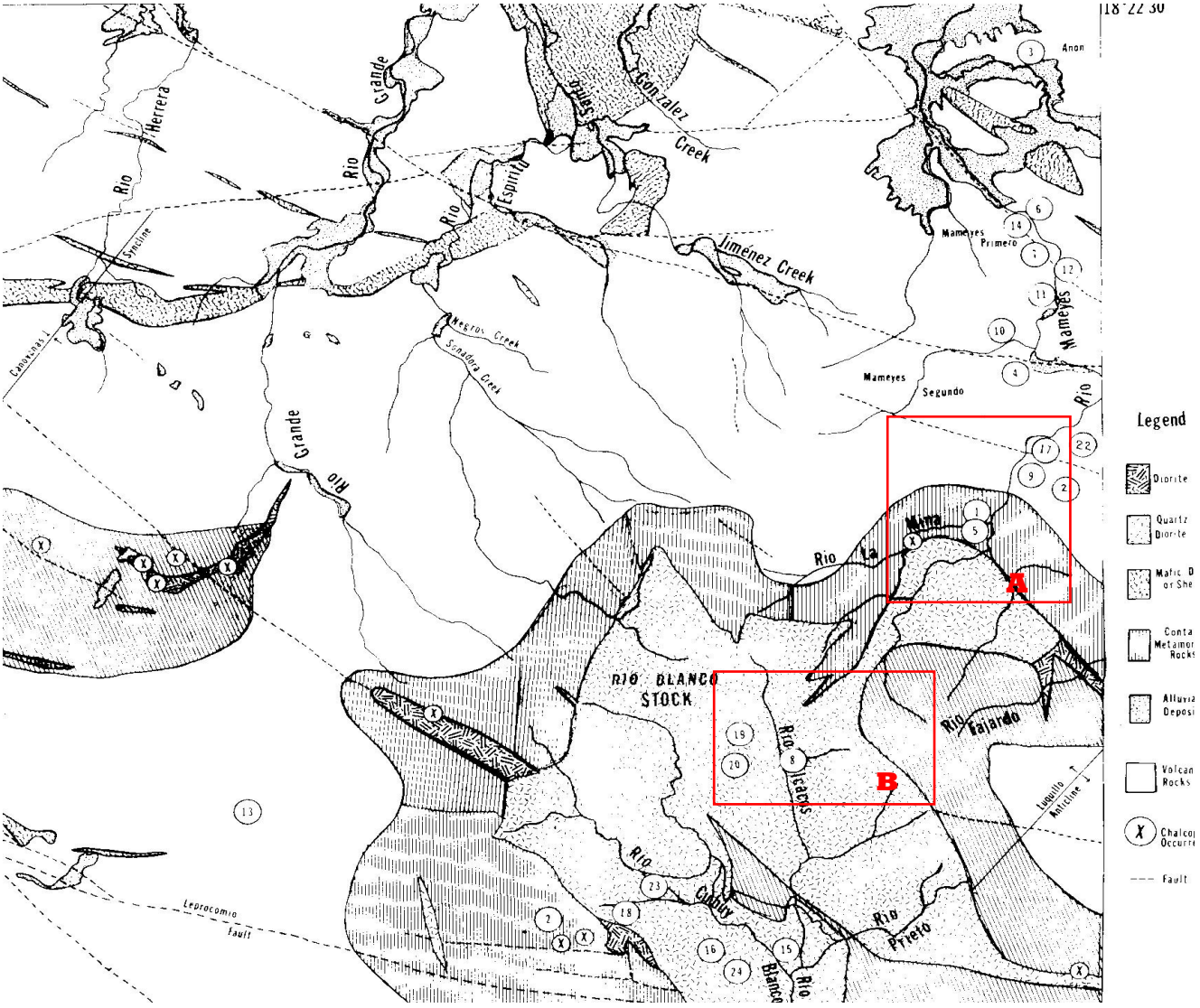

FIGURE 1.3: **Geologic Map of El Yunque Quadrangle, after Seiders (1971)** *Cardona (1984).*

The numbers on the map represent the location of the mines as noted by the Puerto Rico Department of Ores and Mines. *(Cardona 1984).*The red squares on indicate the approximate regions that were sampled in the Luquillo/ El Yunque region. The locations were chosen based on the proximity to the contact zone of metamorphism at La Mina and the USGS study where high Hg levels were found. Region A is underlained by the Fajardo, Tabonuco and Hato Puerco Formations and Region B is underlained by the Rio Blanco Stock.

METHODOLOGY

X-ray Fluorescence

X – Ray fluorescence analyses the atomic composition of a material by irradiating a sample with high energy photons such as x-rays or gamma rays and observing the observing the resulting x-ray fluorescence. *(http.www.erc.carleton.edu/research_education/geochemsheets/techniques/)*

In X-ray fluorescence, the sample is exposed to x-rays or gamma rays and as they hit the sample electrons surrounding the nuclei of the sample atoms are knocked out of their outer orbits. The process in which an x-ray is absorbed by the atom by transferring all of its energy to an innermost electron is called the "photoelectric effect." During this process, if the primary x-ray had sufficient energy, electrons are ejected from the inner shells, creating vacancies. These vacancies present an unstable condition for the atom. As the atom returns to its stable condition, electrons from the outer shells are transferred to the inner shells and in the process give off a characteristic x-ray whose energy is the difference between the two binding energies of the corresponding shells. Because each element has a unique set of energy levels, each element produces x-rays at a unique set of energies, allowing one to non-destructively measure the elemental composition of a sample. The detector collects the spectrum and converts them to electrical impulses; these impulses are proportional to the energies of the various x-rays in the sample's spectrum. Since each element has a different and identifiable x-ray signature, the presence and concentration of the element can be determined by counting the pulses in that sector.

Field Sampling

Field work for this project was conducted in March 2010. The different rock formations in the region were identified from hand specimens and geological maps. The sample sites were chosen based on their proximity to the contact zone at La Mina using the geological map of the El Yunque Quadrangle *(Fig 1.3).*Samples were also taken along the Rio Icacos where high Hg levels were found in the 2007 study done by the USGS. All sediment

samples were bagged and labelled. In situ readings of the rocks were taken in two minute intervals with the use of the XRF machine.

Lab analysis

Field samples were also brought back to the lab at the University of Pennsylvania for further testing in a controlled setting. Sediment samples were subsequently air dried and tested using the XRF with the same time frame as was used in the field. Multiple tests were run in some of the volcanoclastic rocks due to their layers and the average of their values was used.

Statistical Analysis

The results obtained from the XRF analysis were then sorted with the use of Microsoft Excel.They were then analyzed and presented with the use of JMP 8.0.2 statistical program. The partial correlation study used to differentiate the bedrock chemistry was conducted using a Manova model in JMP. Clusters of elements were chosen at random, however a centroid plot was generated only for those that contained highly negative Eigen values which indicated that they were significantly different enough to allow separation. Titanium (Ti) and Iron (Fe) were excluded in these tests because they are present in all rocks and have been concentrated by extensive physical weathering. Elements whose readings were below detection were also not included in this study.

RESULTS

Figures 2.1- 2.4 Shows the XRF analysis for the Unconsolidated Sediment Samples taken from the Luquillo Mountain sample sites. The Unconsolidated Sediments were tested wet and subsequently air dried and re-tested. The wet and dry values for each element were plotted against each other for all of the five formations that were a part of the study. As shown from the graphs below, there is generally a higher concentration of the element in the dried sample as compared to the wet. Although this is expected, as the XRF values represent percentages of the total sample weight, there was no consistent pattern between wet and dry samples, as would

be expected if the difference was simply due to the added weight of water. Thus the wet readings were thought not to be accurate. All subsequent analysis in this study was done with the values from the dried sediments.

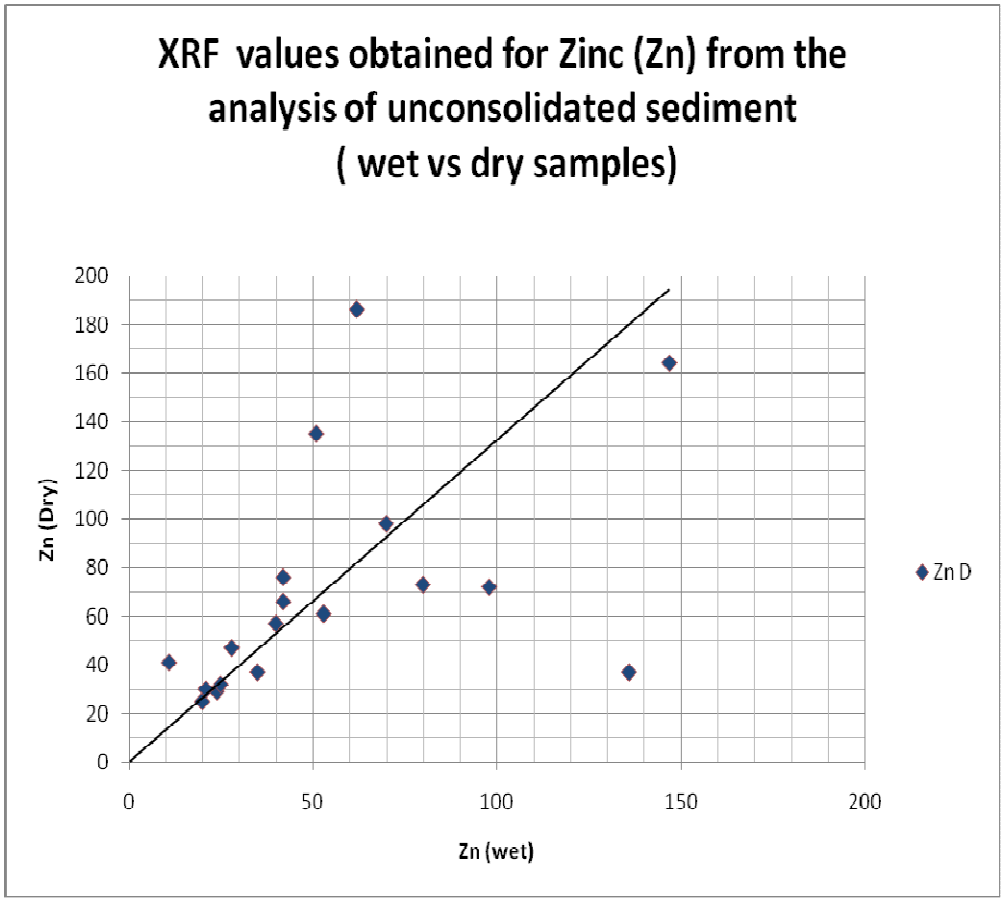

Figure 2.1 Showing the XRF results for wet VS dry values of Zinc (Zn) the unconsolidated alluvial sediments of the Luquillo Mountains.

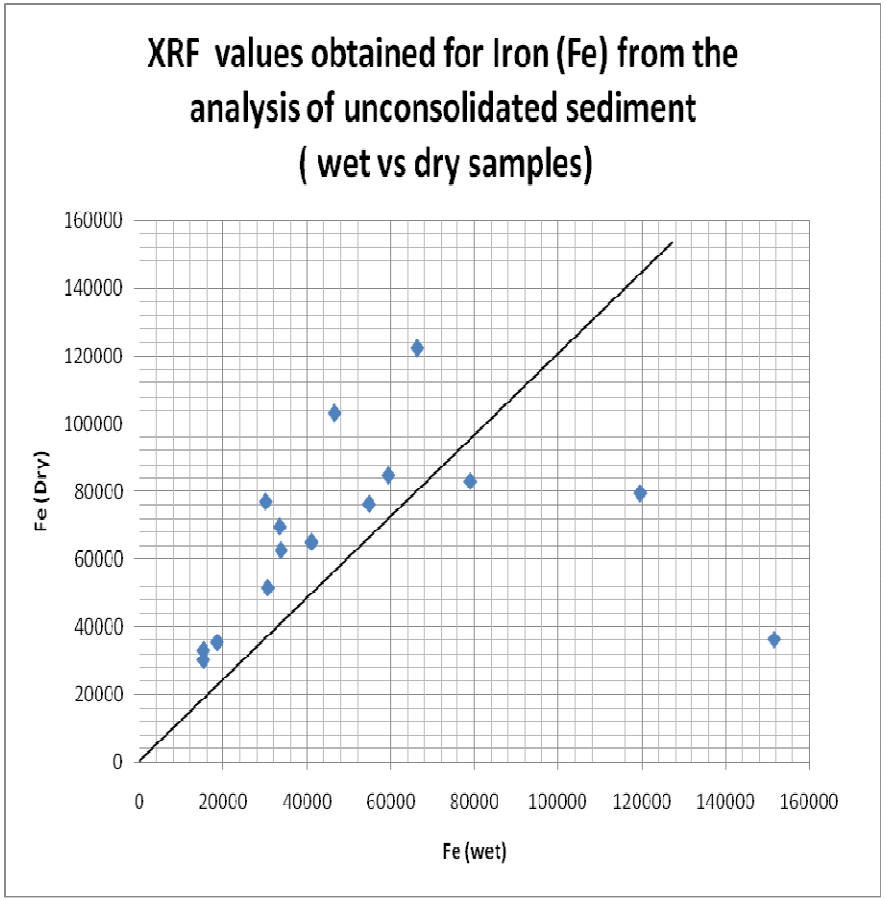

Figure 2.2 Showing the XRF results for wet VS dry values of Iron (Fe) the unconsolidated alluvial sediments of the Luquillo Mountains.

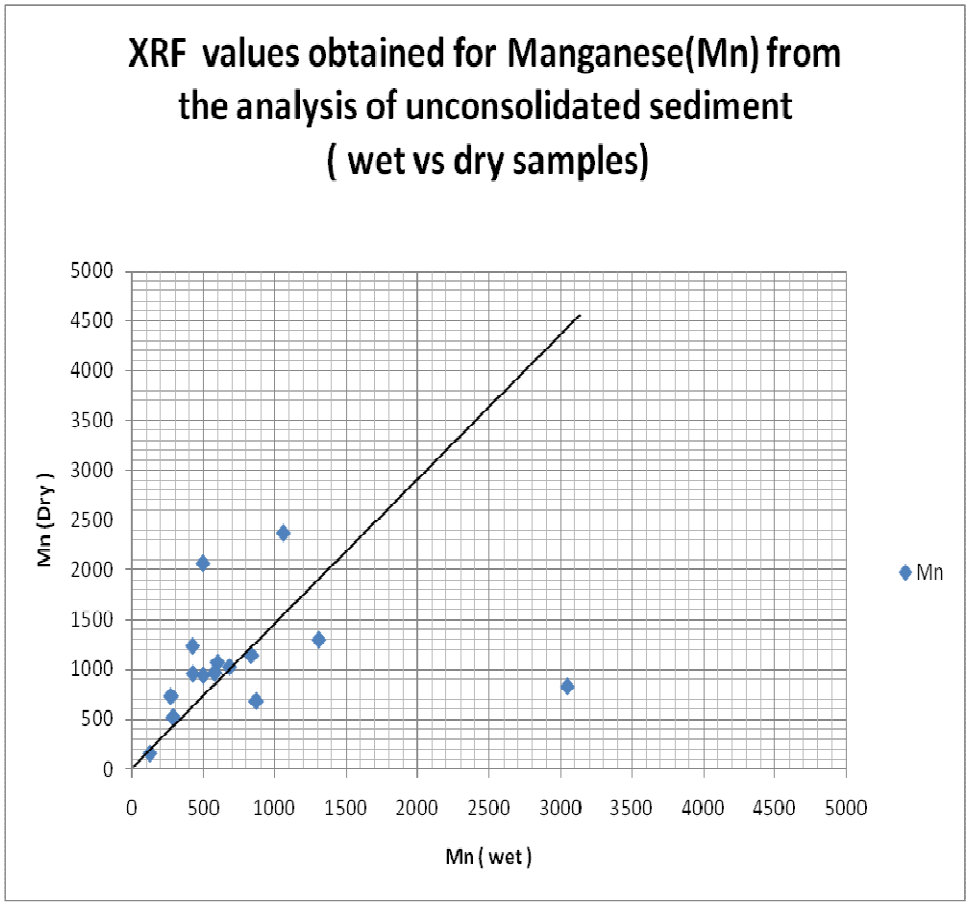

Figure 2.3 Showing the XRF results for wet VS dry values of Manganese (Mn) the unconsolidated alluvial sediments of the Luquillo Mountains.

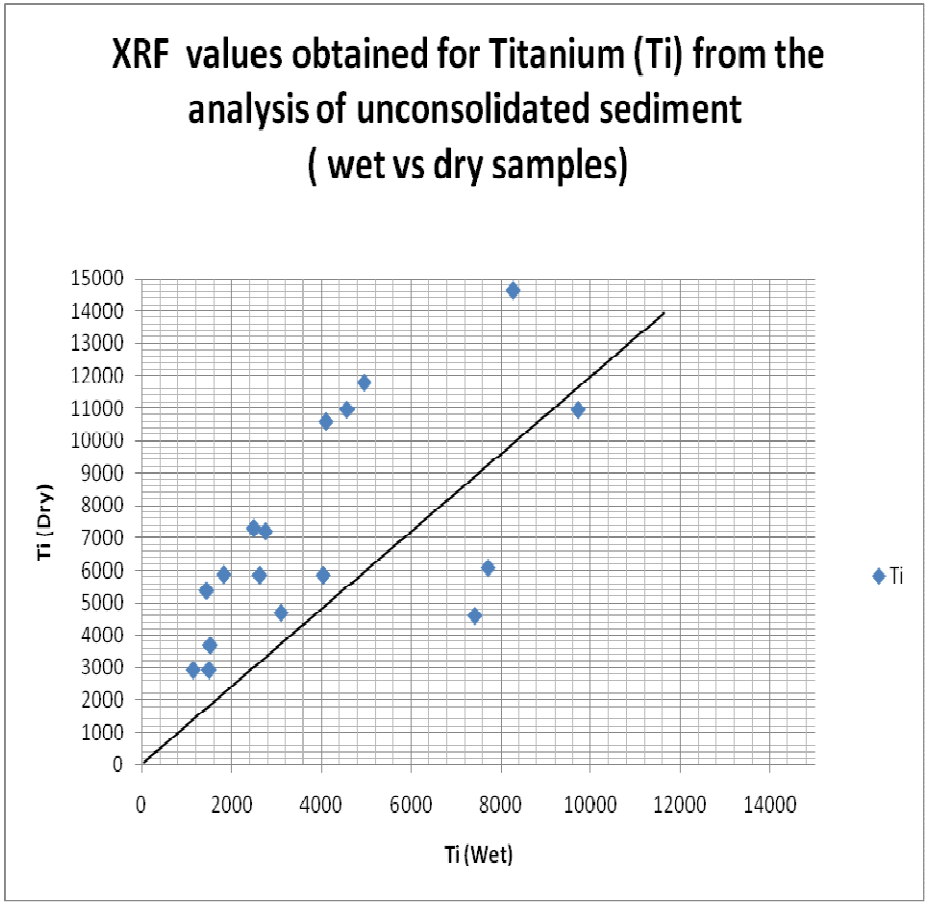

Figure 2.4 Showing the XRF results for wet VS dry values of Titanium (Ti) the unconsolidated alluvial sediments of the Luquillo Mountains.

Table 2.5 The Mean and Standard Deviation for each of the different rock formations and rock types of the Luquillo Mountains.

Formation	Rock type*	No of samples	Mean(Ti)	Std Dev(Ti)	Mean(Cr)	Std Dev(Cr)	Mean(Mn)	Std Dev(Mn)	Mean(Fe)	Std Dev(Fe)
Fajardo	vx	25	3169	4131	116	190	3376	8650	48925	30295
Hato Puerco	ms	31	4485	5021	70	145	1384	1926	93835	125521
Río Blanco	gdx	25	2176	1821	4	22	706	391	30723	13467
Tabonuco	mvx	3	1568	2404	0	0	834	597	37391	20302
Tabonuco	vx	32	3481	3889	298	823	3366	7567	72371	96655
Unnamed	mvx	32	3312	2939	14	39	4871	9516	84554	96282

Formation	Rock type*	No of Samples	Mean(Co)	Std Dev(Co)	Mean(Ni)	Std Dev(Ni)	Mean(Cu)	Std Dev(Cu)	Mean(Zn)	Std Dev(Zn)
Fajardo	vx	25	712	550	52	78	71	49	95	72
Hato Puerco	ms	31	1166	716	2	11	66	68	58	32
Río Blanco	gdx	25	444	171	3	16	20	37	25	10
Tabonuco	mvx	3	707	463	0	0	107	106	59	49
Tabonuco	vx	32	738	426	287	875	64	50	106	139
Unnamed	mvx	32	1029	592	4	15	284	277	78	48

Formation	Rock type*	No of Samples	Mean(As)	Std Dev(As)	Mean(Rb)	Std Dev(Rb)	Mean(Sr)	Std Dev(Sr)	Mean(Zr)	Std Dev(Zr)
Fajardo	vx	25	7	10	24	17	190	123	65	32
Hato Puerco	ms	31	5	15	10	12	392	470	93	103
Río Blanco	gdx	25	0	1	19	7	202	121	67	31
Tabonuco	mvx	3	0	0	25	17	1371	1076	107	8
Tabonuco	vx	32	4	8	12	12	576	552	69	39

			1	3	9	8	212	168	80	41
Unnamed	mvx	32								
Formation	**Rock type***	**No of Samples**	**Mean(Mo)**	**Std Dev(Mo)**	**Mean(Ag)**	**Std Dev(Ag)**	**Mean(Ba)**	**Std Dev(Ba)**	**Mean(Hg)**	**Std Dev(Hg)**
			1	2	19	21	2134	2979	0	2
Fajardo	vx	25								
			2	5	17	21	661	899	1	4
Hato Puerco	ms	31								
			1	2	15	23	290	253	1	3
Río Blanco	gdx	25								
			0	0	12	21	941	194	0	0
Tabonuco	mvx	3								
			3	8	32	21	994	969	3	6
Tabonuco	vx	32								
			5	10	22	21	745	458	3	6
Unnamed	mvx	32								

*Legend: Vx – Volcanoclastics Rocks, Ms – Marine Sediments , gdx – Granodiorite Rock, mvx- Marine Volcanoclastic Rocks

Standard Deviation & Partial Correlation Relationship

The range of means and standard deviation of the elements between the rock types indicates that the different formations can be distinguished on the basis of their elemental chemistry. Fig 2.6: The partial correlation analysis of elements in the different bedrock formations In the Luquillo Mountains. The red arrow indicates the separation of the Fajardo and the Unnamed Formation along the lines of Barium (Ba) and Copper (Cu) respectively the Rio Blanco Formation is located at the center of the separation of the model.

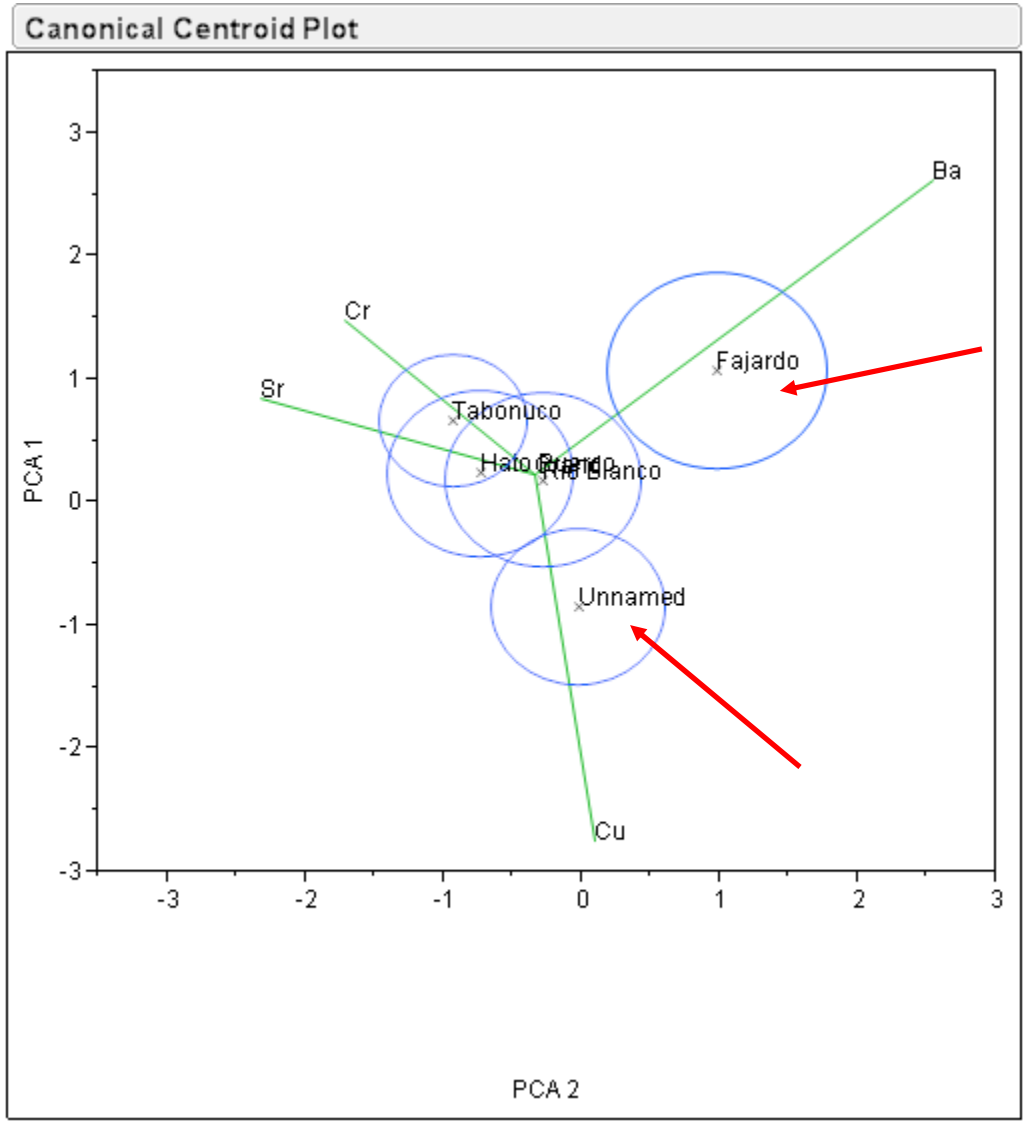

Figure 2.6*- The partial correlation of the 5 formations using Manova fit model. Cr (Chromium)), Sr (Strontium), Ba (Barium), Rb (Rubidium), Cu (Copper) and Hg (Mercury)*

Legend: PCA 1- Principal Components Analysis 1

PCA 2- Principal Component Analysis 2

Figure 2.6- The separation of the 2 of the 5 different formations with the use of a Manova fit model. Cr – Chromium , Sr- Strontium, Ba- Barium, Rb -Rubidium , Cu- Copper. The red arrows indicate the separation of the Unnamed and the Fajardo Formations. The Rio Blanco formation is located in the Nucleus of the formations.

Figure 2.7: The principal components analysis of elements in the different bedrock formations. The Hato Puerto and the Unnamed Formation separated along the lines of Nickel (Ni). The Manova test also shows Tabonuco also beginning to separate from both the Hato Puerco and the Rio Blanco along the line of Strontium (Sr). Fajardo has separated from the other four formations along the lines of Barium (Ba) and Rubidium (Rb) and the Unnamed Formation separated along the lines of Copper (Cu). Mercury (Hg) is present in rocks of the Unnamed Formation.

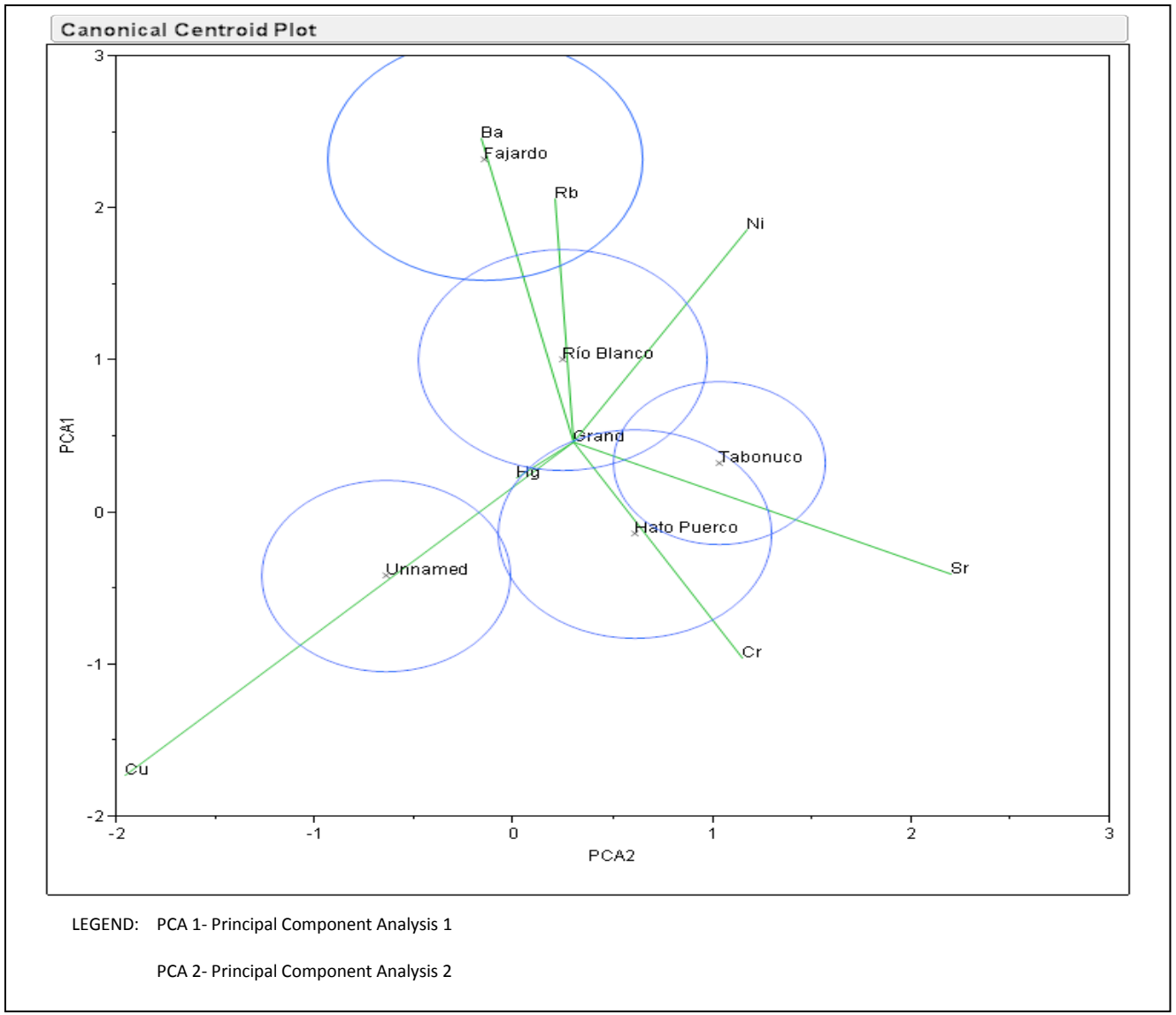

LEGEND: PCA 1- Principal Component Analysis 1

PCA 2- Principal Component Analysis 2

Figure 2.7*- The partial correlation of the 5 formations using Manova fit model taken from JMP 8.0. Cr (Chromium), Sr (Strontium), Ba (Barium), Rb (Rubidium), Cu (Copper) and Hg (Mercury)*

DISCUSSION

Sediment Analysis

Controlled testing of wet and dry sediments indicated that the XRF recorded higher concentrations shows of each of the elements in the dried as compared to the wet sediments *(Figure 2.1 – 2.4)*. When a primary x-ray excitation source from an x-ray tube or a radioactive source strikes a sample, the x-ray can either be absorbed by the atom or scattered through the material. The scattering effect is thought to occur when the X-ray hit the wet samples. The ray is reflected off the water molecule that coats the sediment sample. The readings obtained are not as accurate as the dry samples thus the uses of dry samples are preferred.

Hg was not detected in any of the sediment samples; however it was identified in some rock samples specifically in the Unnamed Formation The possible cause for the lack of mercury in the sediment samples is the intense physical weathering with major landslides that occur in the region. *(Murphy et al 2009)* If Hg had been used in the historic mines it has apparently washed out of the area.

Rock Analysis

The mercury found in the rocks along the Unnamed Formation range in values between 2-6 ppm. The Hg found in the Unnamed Formation and along the La Mina trail is apparently natural and related to hydrothermal alterations during the emplacement of the granodiorite stock. The Granodiorite rocks did not contain any Hg.

The Fajardo Formation separated from the other bedrocks based upon its high Barium (Ba) content. The Fajardo Formation consists of breccias and andesite developed from the subduction of the North American plate under the overriding Caribbean plate. The Fajardo is the oldest of the formations (100-150 Mya) *(Murphy et al 2009)* and was the first that formed after the volcanic activity and the barium was formed due to the melting of the overlying mantle wedge which can be detected by increased lead and barium in the melts which were produced.

The Unnamed Formation separated along the line of Copper (Cu). The Unnamed Formation consists of Cretaceous aged volcanoclastic rocks. The Copper (Cu) found within this formation may be in direct correlation to the deposits southeast of La Mina peak which were worked between 1866 and 1868. (*Cardona, 1984).*

The separation between the Unnamed and the Hato Puerco Formation occurred along the line of the Chromium (Cr). The calcareous Hato Puerco consists of thickly bedded volcanic sandstone that is both andesitic and basaltic in nature which differs from the andesitic non calcareous Fajardo Formation. The most probable origin of the high-alumina basalts was by crystal fractionation from more mafic, mantle-derived primary magmas. Chromium (Cr) and Nickel (Ni) in basaltic rocks *(Turekian, 1963)* has been observed and its preservation is thought to have occur during fractional crystallization of a basaltic magma suggesting preservation of the chromium-nickel ratio from the source of basaltic magma.

The Rio Blanco Formation is the youngest of the formations (35-55 Mya) and its genesis caused the metamorphosis of the Fajardo, Tabonuco and Hato Puerto Formations *(Murphy et al 2009).*Figures 2.The Rio Blanco is located at the nucleus of the separation of the formations which is expected since it is the magma that created the other formations.

SUMMARY

- The XRF machine is most accurate when the samples are dried as compared to wet due to the interaction between the ray and the water molecule on wet samples.
- Mercury (Hg) is not found in the fluvial sediments collected near historic mine sites. It was found in the metamorphosed volcanoclastics rocks near La Mina. La Mina is at the contact zone of the metamorphosis.
- The formations can be separated based upon their geo chemistry with Fajardo separating first, followed by the Unnamed Formation. However not all the formations can be separated by their basic elemental chemistry but are separable on other features such as their mineralogy, stratigraphy and bedrock chemistry.
- The Volcanoclastics had higher amounts of metals such as Titanium, Iron, Barium, and Cobalt as compared to the Granodiorites.

REFERENCES

Brown E, Stallard R, Larsen M, Raisbeck G, Yiou F ; Denudation rates determined from the accumulation of in situ produced Be in the Luquillo Experimental Forest, Puerto Rico (1994)

Brighman, M. et al, Mercury in stream ecosystems- New studies initiated by the US geological survey (2003)

Cardona, W, El Yunque Mineral Prospects of Eastern Puerto Rico (1984)

Christopher Daly, H. Helmer, Maya Quiñones; Mapping the Climate of Puerto Rico, Vieques and Culebra (2002)

Donovan, S; Jackson T 1994: Caribbean Geology An Introduction

Gillespie, M R, and Styles, M T. 1999.BGS Rock Classification Scheme Volume 1Classification of igneous rocks. British Geological Survey Research Report, (2nd edition) RR 99–0

Lugo, A. E. & Brown S, Ecological monitoring in the Luquillo Forest Reserve, Ambio Vol 10 no.2/3 mab: A special issue (1981) pp 102-107

Lugo A, Waide R, Catastrophic and background disturbance of tropical ecosystems at the Luquillo Experimental Forest, 1993

Shanley, J et al, Comparison of total mercury and methylmercury cycling at five sites using the small watershed approach, Environ Pollution (2008)

Murphy Sheila F; Stallard Robert F; Larsen Matthew C; Gould William A; Water Quality and Landscape Processes of Eastern Puerto Rico: A comparison of Four Humid – Tropical Forested and Developed Watersheds. 2009

Scatena, Frederick N. An Introduction to the Physiography and History of the Bisley Experimental Watersheds in the Luquillo Mountains of Puerto Rico (1989)

REFERENCES

Schellekens, J ,F. N. Scatena,L. A. Bruijnzeel, A. I. J. M. van Dijk,M. M. A. Groen and R. J. P. van Hoogezand - Stormflow generation in a small rain-forest catchment in the Luquillo Experimental Forest, Puerto Rico (2003)

Sieders W; Cretaceous and Lower Tertiary Stratigraphy of the Gurabo and El Yunque Quadrangles of Puerto Rico pages F1-F53 (1971)

Warne, Andrew G; Webb, Richard M.T, Larsen Matthew C: Water, Sediment, and Nutrient Discharge Characteristics of Rivers in Puerto Rico, and their Potential Influence (2005)

Webb R M T ; Gomez –Gomez F ; 1998 : Synoptic survey of water quality and bottom sediments , San Juan Bay estuary system , Puerto Rico December 1994- July 1995 US Geological Survey Report 97-414

Mercury Amalgamation : http://corrosion-doctors.org/Elements-Toxic/Mercury-amalgamation.htm assessed April 19th , 2010

http://serc.carleton.edu/research_education/geochemsheets/techniques/XRF.html assessed April 19th 2010

(http.www.erc.carleton.edu/research_education/geochemsheets/techniques/)

APPENDIX 1

Elemental Values for Dried Sediments

Table 3.1 –XRF Values of dried unconsolidated alluvial sediments of the Luquillo Mountains. *Map location A represents the bedrock of the Fajardo, Tabunaco and Hato Puerco Formations and B refers to the bedrock of the Rio Blanco Stock Formation.

Reading	Formation	Map Location	Ti D	Ti (e)	Mn D	Mn (e)	Fe D	Fe (e)	C0 D	C0 (e)	Cu D	Cu (e)
c01_ a	Unnamed	A	7206	434	33778	313	69695	567	1164	77	653	15
c0 1_ b	Unnamed	A	10960	510	31996	319	84843	724	1068	88	769	17
c0 1_c	Unnamed	A	14624	527	5641	98	103192	840	1464	95	170	9
c0 1_d	Unnamed	A	10591	689	828	80	265199	2401	2513	171	324	13
C0 2_e	Rio Blanco	B	2938	259	732	34	33214	265	553	48	0	13
c0 2_f	Rio Blanco	B	4698	308	155	30	51633	396	583	59	21	5
c0 3 _b	Rio Blanco	B	3694	270	1070	38	35547	274	474	48	28	5
c0 5 _c	Fajardo	A	6083	387	1298	52	79552	640	1165	81	50	6
c0 5_ f	Fajardo	A	5860	356	966	43	62737	488	896	68	61	6
c0 7 _1	Fajardo	A	7303	404	941	46	77082	606	1150	78	61	6
c07 a_1	Fajardo	A	5860	391	1026	48	76368	608	1160	79	132	8
c07a_2	Fajardo	A	5383	369	956	44	65097	510	908	70	53	6
c08_g	Hato Puerco	A	11790	529	2371	71	122375	1015	1795	106	199	9
c0 10_ f	Hato Puerco	A	2938	256	518	30	30343	238	433	44	20	5
c0 11_ e	Hato Puerco	A	4606	289	681	33	36395	281	443	49	26	5
c012_ b	Hato Puerco	A	23286	802	2066	88	230598	2082	3432	163	0	20
c0 12_e	Hato Puerco	A	10951	438	1142	49	83108	642	1141	80	36	5
c0 22_ s	Unnamed	A	5879	356	1235	47	52661	433	890	66	148	8

Table 3.1 –XRF Values of dried unconsolidated alluvial sediments of the Luquillo Mountains. *Map location A represents the bedrock of the Fajardo, Tabunaco and Hato Puerco Formations and B refers to the bedrock of the Rio Blanco Stock .

Reading	Formation	Map Location	Zn D	Zn (e)	Rb D	Rb (e)	Sr D	Sr (e)	Zr D	Zr (e)	Ba D	Ba (e)
c01_ a	Unnamed	A	164	7	8	1	6	1	124	2	1360	154
c0 1_ b	Unnamed	A	186	8	3	1	11	1	128	2	1138	172
c0 1_c	Unnamed	A	25	4	6	1	5	1	224	3	748	165
c0 1_d	Unnamed	A	57	6	21	1	11	1	189	3	1811	248
C0 2_e	Rio Blanco	B	29	3	16	1	88	2	79	2		271
c0 2_f	Rio Blanco	B	30	3	8	1	7	1	136	2		314
c0 3 _b	Rio Blanco	B	37	3	22	1	29	1	62	2	304	93
c0 5 _c	Fajardo	A	72	5	12	1	142	3	67	2	486	133
c0 5_ f	Fajardo	A	98	5	19	1	155	3	86	2	669	122
c0 7 _1	Fajardo	A	73	5	15	1	164	3	55	2	881	138
c07 a_1	Fajardo	A	135	6	21	1	151	3	101	2	968	138
c07a_2	Fajardo	A	61	4	16	1	132	2	78	2	1065	131
c08_g	Hato Puerco	A	66	5	36	1	20	1	99	2	1070	175
c0 10_ f	Hato Puerco	A	32	3	6	1	54	1	38	1	393	90
c0 11_ e	Hato Puerco	A	37	3	21	1	29	1	53	2	391	97
c012_ b	Hato Puerco	A	47	5	15	1	30	2	166	3	1816	256
c0 12_e	Hato Puerco	A	41	4	12	1	27	1	620	6	516	139
c0 22_ s	Unnamed	A	76	5	10	1	149	3	94	2	441	119

APPENDIX #2

Elemental Values of the Rock Analysis

Table 3.2 - Showing the XRF Values obtained from the Luquillo Mountain sample sites separated by formation and rock type.

Field ID	formation	Rock type	Ti	Ti +/-	Cr	Cr +/-	Mn	Mn +/-	Fe	Fe +/-	Co	Co +/-
co 5c	Fajardo	vx	7732	488		132	1309	60	119583	989	2036	106
co 5f	Fajardo	vx	2624	237		69	580	30	33802	248	589	45
co 7a	Fajardo	vx	2499	232		68	502	28	30114	223	576	42
co7b	Fajardo	vx	446	32		86	683	36	54846	403	1142	62
co7c	Fajardo	vx	1442	257		77	428	31	41090	317	1063	55
co 5c	Fajardo	vx	683	387		109	1298	52	79552	640	1165	81
co 5f	Fajardo	vx	586	356	0	95	966	43	62737	488	896	68
co 7a	Fajardo	vx	733	44		108	941	46	77082	606	1150	78
co 7b	Fajardo	vx	586	391	110	36	1026	48	76368	608	1160	79
co 7c	Fajardo	vx	5383	369		101	956	44	65097	510	908	70
co 5a	Fajardo	vx	929	24	135	26	98	24	33917	255	0	129
co 5b	Fajardo	vx	2577	342	96	30	506	33	27470	245	725	49
co 5d	Fajardo	vx	4126	34	0	96	1978	57	49557	429	442	65
co 5d_1	Fajardo	vx	1532	223	0	64	346	25	13129	132	184	32
co 5e	Fajardo	vx	587	422	0	116	920	51	62899	595	818	82
co 5f	Fajardo	vx	19814	628	443	46	1618	55	72461	577	699	75
co 5g	Fajardo	vx	232	36	0	89	908	39	49655	379	0	167
co 4a	Fajardo	vx	917	249	0	74	924	35	20781	181	111	37
co 4b	Fajardo	vx	1639	442	306	36	13082	129	7323	84	747	28
co 4c	Fajardo	vx	179	295	204	27	470	27	19541	159	137	33
co 4d	Fajardo	vx	4813	313	227	28	419	28	24473	197	309	39
co 4e	Fajardo	vx	5264	45	216	35	8796	108	41476	324	278	52
co 4f	Fajardo	vx	2183	568	420	49	42529	342	16367	159	285	35
co 5c	Fajardo	vx	7732	488	0	132	1309	60	119583	989	2036	106
co 6a	Fajardo	vx	3994	386	745	42	1797	50	24228	215	353	43

Field ID	Formation	Rock type	Ni	Ni +/-	Cu	Cu +/-	Zn	Zn +/-	As	As +/-	Rb	Rb +/-
co 5c	Fajardo	vx		61	72	7	98	6	11	2	7	1
co 5f	Fajardo	vx		38	47	5	70	4	5	1	12	1
co 7a	Fajardo	vx		35	63	5	80	4	14	2	10	1
co7b	Fajardo	vx		43	41	5	51	4		4	9	1
co7c	Fajardo	vx		42	44	5	53	4	4	1	8	1
co 5c	Fajardo	vx		52	50	6	72	5		5	12	1
co 5f	Fajardo	vx	0	46	61	6	98	5	7	2	19	1
co 7a	Fajardo	vx		52	61	6	73	5	7	2	15	1
co 7b	Fajardo	vx		51	132	8	135	6	28	2	21	1
co 7c	Fajardo	vx		48	53	6	61	4		5	16	1
co 5a	Fajardo	vx	75	13	28	5	57	4	4	1	14	1
co 5b	Fajardo	vx	0	45	89	7	38	4	0	5	32	1
co 5d	Fajardo	vx	0	48	0	16	47	4	0	5	46	2
co 5d_1	Fajardo	vx	0	38	0	13	0	8	0	4	14	1
co 5e	Fajardo	vx	0	58	76	8	52	5	0	5	22	1
co 5f	Fajardo	vx	76	18	75	7	129	6	14	2	51	2
co 5g	Fajardo	vx	156	16	79	6	88	5	10	2	16	1
co 4a	Fajardo	vx	84	14	72	6	98	5	0	4	28	1
co 4b	Fajardo	vx	201	15	64	6	92	4	8	2	17	1
co 4c	Fajardo	vx	51	12	79	6	95	4	6	1	30	1
co 4d	Fajardo	vx	68	13	194	8	261	7	5	2	68	2
co 4e	Fajardo	vx	157	16	185	8	349	8	40	4	68	2
co 4f	Fajardo	vx	159	15	144	7	129	5	0	5	30	1
co 5c	Fajardo	vx	0	61	72	7	98	6	11	2	7	1
co 6a	Fajardo	vx	266	18	0	16	42	4	0	5	18	1

Field ID	Formation	Rock type	Sr	Sr +/-	Zr	Zr +/-	Mo	Mo +/-	Ag	Ag +/-	Ba	Ba +/-	Hg	Hg +/-
co 5c	Fajardo	vx	96	2	106	2		6		27	1454	173		9
co 5f	Fajardo	vx	110	2	48	2		5		21	253	84		7
co 7a	Fajardo	vx	103	2	55	2	8	2		21	331	83		6
co7b	Fajardo	vx	118	2	100	2		5		23	535	107		7
co7c	Fajardo	vx	232	3	45	2		5		23	580	98		8
co 5c	Fajardo	vx	142	3	67	2		6		26	486	133		9
co 5f	Fajardo	vx	155	3	86	2	0	6	0	24	669	122	0	8
co 7a	Fajardo	vx	164	3	55	2		6	39	8	881	138		9
co 7b	Fajardo	vx	151	3	101	2	7	2		25	968	138		9
co 7c	Fajardo	vx	132	2	78	2		6		25	1065	131		9
co 5a	Fajardo	vx	90	2	33	1	0	5	36	7	840	94	0	7
co 5b	Fajardo	vx	604	6	95	2	0	6	36	8	2100	132	0	8
co 5d	Fajardo	vx	276	4	25	2	0	6	0	26	389	119	11	3
co 5d_1	Fajardo	vx	278	4	31	2	0	6	0	24	0	241	0	8
co 5e	Fajardo	vx	258	4	60	2	0	7	41	10	762	148	0	10
co 5f	Fajardo	vx	254	4	152	3	0	6	55	9	4885	210	0	9
co 5g	Fajardo	vx	89	2	36	2	0	5	46	8	1396	118	0	7
co 4a	Fajardo	vx	94	2	37	2	0	5	40	8	1046	98	0	8
co 4b	Fajardo	vx	192	3	26	1	0	5	45	7	8957	192	0	7
co 4c	Fajardo	vx	102	2	36	1	0	5	25	7	2947	121	0	7
co 4d	Fajardo	vx	197	3	78	2	0	5	0	22	1536	112	0	8
co 4e	Fajardo	vx	167	3	84	2	0	5	46	8	3556	154	0	9
co 4f	Fajardo	vx	161	2	41	2	0	5	40	8	13101	253	0	8
co 5c	Fajardo	vx	96	2	106	2	0	6	0	27	1454	173	0	9
co 6a	Fajardo	vx	479	5	42	2	0	6	37	8	3159	150	0	7

Field ID	Formation	Rock type	Ti	Ti +/-	Cr	Cr +/-	Mn	Mn +/-	Fe	Fe +/-	Co	Co +/-
co 8g	Hato Puerco	ms	4959	345		93	1062	45	66349	512	1172	71
co 10f	Hato Puerco	ms	1155	175		53	290	21	15278	127	296	30
co 11e	Hato Puerco	ms	7431	529	379	55	869	62	151601	1301	2276	124
co 12b	Hato Puerco	ms	3529	268		74	500	30	36415	279	685	50
co 12e	Hato Puerco	ms	9738	428		106	836	45	78994	624	1424	81
co 8g	Hato Puerco	ms	1179	529		135	2371	71	122375	1015	1795	106
co 10f	Hato Puerco	ms	2938	256		73	518	30	30343	238	433	44
co 11e	Hato Puerco	ms	23286	82		190	2066	88	230598	2082	3432	163
co 12b	Hato Puerco	ms	1951	438		103	1142	49	83108	642	1141	80
co 12e	Hato Puerco	ms	466	289	0	74	681	33	36395	281	443	49
co 8a	Hato Puerco	ms	16613	1372	673	150	11414	267	728686	8836	3216	368
co 8c	Hato Puerco	ms	6951	872	0	243	875	101	86209	1456	1100	177
co 8d	Hato Puerco	ms	1422	633	0	145	1402	69	108593	1053	1319	115
co 9a	Hato Puerco	ms	7414	472	0	127	1439	62	109627	945	1330	103
co 10a	Hato Puerco	ms	3197	359	175	38	825	47	47122	459	1083	74
co 10b	Hato Puerco	ms	5124	459	149	45	689	54	63376	679	1036	93
co 10c	Hato Puerco	ms	6396	417	0	112	815	48	68099	602	1124	82
co 10d	Hato Puerco	ms	5443	381	0	108	774	45	62502	533	1044	75
co 10e	Hato Puerco	ms		716	0	78	1299	45	19605	196	790	46
co 11a	Hato Puerco	ms	548	387	165	38	1732	58	67380	577	842	78
co 11b	Hato Puerco	ms	4912	329	0	88	548	36	32908	298	563	54
co 11c	Hato Puerco	ms	667	438	0	122	1029	55	71280	672	1317	90
co 11d	Hato Puerco	ms	891	293	141	34	994	45	45804	402	545	63
co 11f	Hato Puerco	ms	6943	41	161	36	1591	54	48273	431	759	67
co 11g	Hato Puerco	ms	5419	457	0	134	1806	70	89364	868	886	101
co 11h	Hato Puerco	ms	7	431	145	41	1629	60	78291	683	1131	87
co 11i	Hato Puerco	ms	359	377	191	42	799	51	60559	602	1057	85
co 11j	Hato Puerco	ms	3335	372	0	108	788	48	46867	476	670	74
co 11k	Hato Puerco	ms	1179	298	0	93	467	37	33765	330	591	59
co 8b	Hato Puerco	ms	5567	393	0	110	682	45	66187	575	934	78

co 8e	Hato Puerco	ms	19	543	0	132	964	59	122929	1074	1708	112

Field ID	Formation	Rock type	Ni	Ni +/-	Cu	Cu +/-	Zn	Zn +/-	As	As +/-	Rb	Rb +/-
co 8g	Hato Puerco	ms		48	109	7	42	4	38	2	18	1
co 10f	Hato Puerco	ms		32		11	25	3		3	5	1
co 11e	Hato Puerco	ms		68	47	7	136	7		6	9	1
co 12b	Hato Puerco	ms		39		13	28	3		4	15	1
co 12e	Hato Puerco	ms		49		15	11	3		4	4	1
co 8g	Hato Puerco	ms	0	61	199	9	66	5	77	3	36	1
co 10f	Hato Puerco	ms		38	20	5	32	3		4	6	1
co 11e	Hato Puerco	ms		82		20	47	5		7	15	1
co 12b	Hato Puerco	ms		51	36	5	41	4	6	2	12	1
co 12e	Hato Puerco	ms	0	41	26	5	37	3	0	4	21	1
co 8a	Hato Puerco	ms	0	165	143	14	152	11	0	16	53	3
co 8c	Hato Puerco	ms	0	114	59	13	105	11	0	11	11	2
co 8d	Hato Puerco	ms	0	70	129	9	73	6	0	6	22	1
co 9a	Hato Puerco	ms	0	62	205	10	84	6	0	6	14	1
co 10a	Hato Puerco	ms	0	57	59	7	63	6	0	5	0	3
co 10b	Hato Puerco	ms	0	67	50	8	45	6	0	6	0	3
co 10c	Hato Puerco	ms	0	57	127	8	62	5	0	5	0	3
co 10d	Hato Puerco	ms	0	53	52	6	59	5	0	5	0	3
co 10e	Hato Puerco	ms	0	48	36	6	16	4	0	5	8	1
co 11a	Hato Puerco	ms	0	56	72	7	68	5	0	5	0	3
co 11b	Hato Puerco	ms	0	47	0	14	56	5	0	5	0	3
co 11c	Hato Puerco	ms	0	60	90	8	51	5	0	5	4	1
co 11d	Hato Puerco	ms	0	51	0	16	36	4	9	2	29	1
co 11f	Hato Puerco	ms	60	18	0	17	113	6	15	2	0	3
co 11g	Hato Puerco	ms	0	65	95	9	45	6	6	2	0	3
co 11h	Hato Puerco	ms	0	60	126	8	58	5	0	5	0	3

co 11i	Hato Puerco	ms	0	61	0	19	42	5	0	6	0	3
co 11j	Hato Puerco	ms	0	57	71	8	38	5	6	2	0	3
co 11k	Hato Puerco	ms	0	51	0	17	31	4	0	6	13	1
co 8b	Hato Puerco	ms	0	56	43	6	58	5	0	5	4	1
co 8e	Hato Puerco	ms	0	65	252	11	69	6	6	2	14	1

Field ID	**Formation**	**Rock type**	**Sr**	**Sr +/-**	**Zr**	**Zr +/-**	**Mo**	**Mo +/-**	**Ag**	**Ag +/-**	**Ba**	**Ba +/-**	**Hg**	**Hg +/-**
co 8g	Hato Puerco	ms	10	1	63	2		6		24	609	121		8
co 10f	Hato Puerco	ms	44	1	27	1	6	2		20		189		6
co 11e	Hato Puerco	ms	192	3	81	2		7	33	9	1413	192		11
co 12b	Hato Puerco	ms	27	1	110	2		5		22	285	93		7
co 12e	Hato Puerco	ms	24	1	53	2	8	2		25	579	138		7
co 8g	Hato Puerco	ms	20	1	99	2	9	2	0	27	1070	175		10
co 10f	Hato Puerco	ms	54	1	38	1		5		22	393	90		7
co 11e	Hato Puerco	ms	30	2	166	3	8	2		30	1816	256		11
co 12b	Hato Puerco	ms	27	1	620	6		6		25	516	139		8
co 12e	Hato Puerco	ms	29	1	53	2	0	5	24	8	391	97		8
co 8a	Hato Puerco	ms	119	4	163	4	23	3	0	42	4824	519	0	18
co 8c	Hato Puerco	ms	546	13	67	5	0	13	0	54	0	901		21
co 8d	Hato Puerco	ms	304	5	90	3	0	7	0	32	1120	203	0	11
co 9a	Hato Puerco	ms	327	5	75	2	0	6	0	28	745	163	0	10
co 10a	Hato Puerco	ms	376	5	53	2	0	7	50	10	0	387	0	10
co 10b	Hato Puerco	ms	355	6	56	3	0	8	48	11	0	476	0	11
co 10c	Hato Puerco	ms	447	6	67	2	0	6	28	9	585	142	0	9
co 10d	Hato Puerco	ms	461	5	69	2	0	6	50	9	551	132	0	9
co 10e	Hato Puerco	ms	2554	22	26	3	8	2	0	26	325	95	0	8
co 11a	Hato Puerco	ms	529	6	83	2	0	6	45	9	637	136	0	9
co 11b	Hato Puerco	ms	431	5	118	3	0	6	46	9	0	326	0	9
co 11c	Hato Puerco	ms	424	6	57	2	0	7	41	10	481	150	0	11

co 11d	Hato Puerco	ms	401	5	111	3	0	6	54	9	595	115	0	9
co 11f	Hato Puerco	ms	586	7	93	3	0	6	33	9	603	133	10	3
co 11g	Hato Puerco	ms	353	5	47	2	0	7	0	31	0	479	0	10
co 11h	Hato Puerco	ms	463	6	71	2	0	6	0	28	494	146	0	9
co 11i	Hato Puerco	ms	567	7	65	3	0	7	0	31	0	408	0	10
co 11j	Hato Puerco	ms	1024	12	85	3	0	7	0	31	0	396	0	10
co 11k	Hato Puerco	ms	704	8	40	2	0	7	43	10	492	114	21	4
co 8b	Hato Puerco	ms	411	5	57	2	0	6	29	9	541	136	0	10
co 8e	Hato Puerco	ms	307	4	76	2	10	2	0	29	1432	186	0	10

Field ID	Formation	Rock type	Ti	Ti +/-	Cr	Cr +/-	Mn	Mn +/-	Fe	Fe +/-	Co	Co +/-
co 2e	Río Blanco	gdx	1497	164		49	274	19	15294	113	271	27
co 2f	Río Blanco	gdx	319	249		69	127	23	30629	238	385	44
co 3b	Río Blanco	gdx	1522	189		55	599	26	18530	144	342	32
co 3a	Río Blanco	gdx	2318	286	0	81	625	36	26985	254	358	49
co 3c	Río Blanco	gdx	2275	25	0	71	523	30	20623	186	313	39
co 3d	Río Blanco	gdx	211	26	0	72	603	32	25719	224	392	44
co 3e	Río Blanco	gdx	2591	254	0	72	440	28	19931	181	276	38
co 3f	Río Blanco	gdx	8315	429	0	107	2126	62	71754	602	971	79
co 12d	Río Blanco	gdx	1219	281	111	28	637	34	7847	105	174	29
co 12f	Río Blanco	gdx	697	345	0	87	817	39	47271	381	650	60
co 12g	Río Blanco	gdx	3519	298	0	80	758	37	25748	238	431	47
co 12h	Río Blanco	gdx	1396	217	0	65	418	26	14486	138	245	33
co 13a	Río Blanco	gdx	1868	268	0	77	522	32	21219	206	289	43
co 13b	Río Blanco	gdx	281	257	0	73	478	30	23692	211	324	42
co 21a	Río Blanco	gdx	3337	298	0	84	1053	41	39724	330	475	55
co 2a	Río Blanco	gdx	436	321	0	85	717	38	41299	351	462	57
co 2g	Río Blanco	gdx	3441	328	0	89	626	39	31151	306	620	57
co 2h	Río Blanco	gdx	38	328	0	93	744	41	35373	330	587	59

co 2i	Río Blanco	gdx	2569	262	0	71	696	33	24145	211	373	43
co 2j	Río Blanco	gdx	2311	288	0	82	1059	43	36227	322	494	56
co 3b	Río Blanco	gdx	166	437	0	120	1002	65	33051	457	423	82
co 12c	Río Blanco	gdx	2737	285	0	84	861	39	36992	316	647	55
co 2e	Río Blanco	gdx	2938	259	0	72	732	34	33214	265	553	48
co 2f	Río Blanco	gdx	4698	38		84	155	30	51633	396	583	59
co 3b	Río Blanco	gdx	3694	27		72	1070	38	35547	274	474	48

Field ID	**Formation**	**Rock type**	**Ni**	**Ni +/-**	**Cu**	**Cu +/-**	**Zn**	**Zn +/-**	**As**	**As +/-**	**Rb**	**Rb +/-**
co 2e	Río Blanco	gdx		29		10	24	2		3	8	1
co 2f	Río Blanco	gdx		37		13	21	3		4	5	1
co 3b	Río Blanco	gdx		33		11	35	3		3	19	1
co 3a	Río Blanco	gdx	0	46	18	5	12	3	0	5	21	1
co 3c	Río Blanco	gdx	0	40	0	13	26	3	0	4	24	1
co 3d	Río Blanco	gdx	0	41	22	5	21	3	4	1	30	1
co 3e	Río Blanco	gdx	0	41	0	13	17	3	0	4	21	1
co 3f	Río Blanco	gdx	0	53	37	6	59	5	6	2	13	1
co 12d	Río Blanco	gdx	81	16	49	7	38	4	0	5	21	1
co 12f	Río Blanco	gdx	0	46	23	5	33	4	0	4	18	1
co 12g	Río Blanco	gdx	0	44	0	14	22	4	0	4	29	1
co 12h	Río Blanco	gdx	0	39	180	8	15	3	0	4	26	1
co 13a	Río Blanco	gdx	0	44	32	6	13	3	0	4	14	1
co 13b	Río Blanco	gdx	0	42	0	15	12	3	0	4	17	1
co 21a	Río Blanco	gdx	0	46	0	13	30	4	0	4	27	1
co 2a	Río Blanco	gdx	0	46	19	5	25	4	0	5	22	1
co 2g	Río Blanco	gdx	0	48	0	16	13	4	0	5	16	1
co 2h	Río Blanco	gdx	0	49	50	6	24	4	0	5	31	1
co 2i	Río Blanco	gdx	0	41	0	13	15	3	0	4	18	1
co 2j	Río Blanco	gdx	0	47	0	14	24	4	0	5	17	1

co 3b	Río Blanco	gdx	0	69	0	23	24	5	0	7	11	2
co 12c	Río Blanco	gdx	0	45	22	5	26	4	0	4	12	1
co 2e	Río Blanco	gdx	0	39		13	29	3	0	4	16	1
co 2f	Río Blanco	gdx		44	21	5	30	3		4	8	1
co 3b	Río Blanco	gdx		39	28	5	37	3		4	22	1

Field ID	**Formation**	**Rock type**	**Sr**	**Sr +/-**	**Zr**	**Zr +/-**	**Mo**	**Mo +/-**	**Ag**	**Ag +/-**	**Ba**	**Ba +/-**	**Hg**	**Hg +/-**
co 2e	Río Blanco	gdx	44	1	49	1	5	1		18		174		5
co 2f	Río Blanco	gdx	11	1	147	2		5		22		258		6
co 3b	Río Blanco	gdx	25	1	39	1		5		20		205		6
co 3a	Río Blanco	gdx	202	3	81	2	0	6	0	26	404	103	0	9
co 3c	Río Blanco	gdx	288	4	61	2	0	6	40	8	305	89	0	8
co 3d	Río Blanco	gdx	221	3	98	2	0	6	0	24	445	94		8
co 3e	Río Blanco	gdx	282	4	46	2	0	6	35	8	302	89	0	8
co 3f	Río Blanco	gdx	261	4	23	2	0	6	39	9	635	141	0	10
co 12d	Río Blanco	gdx	567	7	55	2	0	6	89	9	896	108	10	3
co 12f	Río Blanco	gdx	187	3	121	2	0	6	0	24	473	115	0	9
co 12g	Río Blanco	gdx	213	3	64	2	0	6	40	9	402	103	0	8
co 12h	Río Blanco	gdx	238	3	47	2	0	5	0	23	0	239	8	3
co 13a	Río Blanco	gdx	262	4	44	2	0	6	36	9	407	98	0	9
co 13b	Río Blanco	gdx	235	3	71	2	0	6	0	24	405	93	0	8
co 21a	Río Blanco	gdx	280	4	49	2	0	6	37	8	410	105	0	8
co 2a	Río Blanco	gdx	196	3	69	2	0	6	0	25	348	110	0	8
co 2g	Río Blanco	gdx	162	3	53	2	8	2	0	28	0	341	0	10
co 2h	Río Blanco	gdx	258	4	88	2	0	6	28	9	577	118	0	9
co 2i	Río Blanco	gdx	264	3	60	2	0	6	0	24	389	93	0	8
co 2j	Río Blanco	gdx	234	3	41	2	0	6	0	26	0	312	0	9
co 3b	Río Blanco	gdx	232	5	42	3	0	9	0	40	548	163	0	13
co 12c	Río Blanco	gdx	268	4	54	2	0	6	42	8	0	304	0	8

co 2e	Río Blanco	gdx	88	2	79	2	0	5	0	23		271	9	3
co 2f	Río Blanco	gdx	7	1	136	2		6		23		314		8
co 3b	Río Blanco	gdx	29	1	62	2		5		22	304	93		7

Field ID	Formation	Rock type	Ti	Ti +/-	Cr	Cr +/-	Mn	Mn +/-	Fe	Fe +/-	Co	Co +/-
co 18a	Tabonuco	mvx	4336	48	0	114	1403	56	60829	553	1238	80
co 19a	Tabonuco	mvx	368	316	0	82	887	39	25273	236	387	47
co 20a	Tabonuco	mvx		882	0	89	213	30	26071	257	496	51
co 23a	Tabonuco	vx	2411	33	119	31	553	35	28419	261	497	50
co 23b	Tabonuco	vx	1141	372	0	129	857	55	107821	939	1253	103
co 23c	Tabonuco	vx	5542	435	170	43	1061	54	78178	703	1210	90
co 23d	Tabonuco	vx		857	2652	70	1684	57	66171	528	1265	74
co 23e	Tabonuco	vx	5472	4	0	95	338	32	30082	275	474	51
co 23f	Tabonuco	vx	329	362	0	89	299	29	18494	189	309	42
co 17a	Tabonuco	vx	3612	389	141	41	1549	60	63636	603	772	82
co 17b	Tabonuco	vx	4967	48	146	40	677	47	58528	556	1104	82
co 18b	Tabonuco	vx	2579	41	0	132	749	55	122753	1042	1302	107
co 23a	Tabonuco	vx		1374	0	159	883	66	179928	1549	518	129
co 23e	Tabonuco	vx		822	1304	52	659	43	65859	520	1445	74
co 23e_1	Tabonuco	vx		983	3853	87	1437	60	87867	709	1485	87
co 22s	Tabonuco	vx	1829	191		55	426	23	20174	148	382	32
co 22s	Tabonuco	vx	5879	356		93	1235	47	52661	433	890	66
co 15a	Tabonuco	vx	1119	246	79	24	344	25	8282	97	82	26
co 14a	Tabonuco	vx	647	469	168	45	1073	57	80544	760	1270	95
co 14b	Tabonuco	vx	11119	68	0	163	12662	188	111036	1086	1083	115
co 14c	Tabonuco	vx	3518	289	88	28	3756	64	45030	331	840	54
co 14d	Tabonuco	vx		3231	0	391	30819	506	563179	7238	0	995
co 14e	Tabonuco	vx	18616	583	210	40	1676	57	56522	503	788	73
co 14f	Tabonuco	vx	2249	326	141	32	397	33	22891	231	404	48

co 14g	Tabonuco	vx	1858	33	147	32	7982	103	41532	327	692	55
co 14h	Tabonuco	vx	5477	376	0	98	1062	47	38610	365	575	62
co 15a	Tabonuco	vx	1169	32	0	99	30456	249	30230	238	0	124
co 16a	Tabonuco	vx	5969	329	0	83	691	35	39112	314	672	54
co 16b	Tabonuco	vx	482	343	0	96	782	42	45109	399	797	64
co 16c	Tabonuco	vx	7161	568	221	48	770	51	81334	710	1082	88
co 16d	Tabonuco	vx	3548	371	0	100	507	41	31616	342	501	62
co 16e	Tabonuco	vx	6591	423	0	108	656	43	52523	479	763	72
co 16f	Tabonuco	vx	5941	425	0	107	483	41	45247	431	780	69
co 16g	Tabonuco	vx	1943	27	0	78	516	31	15562	162	186	37
co 16h	Tabonuco	vx	224	333	98	32	680	39	26928	269	206	50

Field ID	**Formation**	**Rock type**	**Ni**	**Ni +/-**	**Cu**	**Cu +/-**	**Zn**	**Zn +/-**	**As**	**As +/-**	**Rb**	**Rb +/-**
co 18a	Tabonuco	mvx	0	58	62	7	114	6	6	0	5	10
co 19a	Tabonuco	mvx	0	44	228	9	41	4	4	0	5	20
co 20a	Tabonuco	mvx	0	51	31	6	21	4	4	0	6	44
co 23a	Tabonuco	vx	52	16	63	6	93	5	5	0	5	17
co 23b	Tabonuco	vx	0	65	140	9	155	7	7	0	6	12
co 23c	Tabonuco	vx	0	61	80	8	59	5	5	0	6	34
co 23d	Tabonuco	vx	3483	49	0	27	38	4	4	0	4	0
co 23e	Tabonuco	vx	0	49	36	6	41	4	4	0	5	10
co 23f	Tabonuco	vx	0	47	28	6	54	5	5	0	6	18
co 17a	Tabonuco	vx	0	61	54	7	55	5	5	0	6	6
co 17b	Tabonuco	vx	0	60	52	7	39	5	5	8	2	0
co 18b	Tabonuco	vx	0	64	108	8	68	5	5	8	2	0
co 23a	Tabonuco	vx	0	74	112	8	234	9	9	0	6	12
co 23e	Tabonuco	vx	2374	40	0	24	26	4	4	0	4	0
co 23e_1	Tabonuco	vx	2931	46	40	9	57	5	5	0	4	0
co 22s	Tabonuco	vx		32	85	5	42	3	3		3	6

co 22s	Tabonuco	vx		47	148	8	76	5	5		5	10
co 15a	Tabonuco	vx	0	39	0	15	28	4	4	0	4	5
co 14a	Tabonuco	vx	0	63	153	9	66	6	6	0	6	44
co 14b	Tabonuco	vx	0	73	35	7	102	7	7	7	2	11
co 14c	Tabonuco	vx	0	42	94	6	99	4	4	0	4	6
co 14d	Tabonuco	vx	0	147	67	12	59	9	9	0	16	15
co 14e	Tabonuco	vx	0	55	54	7	140	7	7	34	3	6
co 14f	Tabonuco	vx	102	17	139	8	777	15	15	0	5	35
co 14g	Tabonuco	vx	130	16	177	8	259	7	7	10	2	42
co 14h	Tabonuco	vx	0	50	0	16	34	4	4	0	5	20
co 15a	Tabonuco	vx	127	14	70	6	274	7	7	5	1	2
co 16a	Tabonuco	vx	0	44	47	6	54	4	4	6	1	4
co 16b	Tabonuco	vx	0	51	0	16	115	6	6	0	5	6
co 16c	Tabonuco	vx	0	60	35	6	67	5	5	20	2	0
co 16d	Tabonuco	vx	0	58	0	18	42	5	5	17	2	7
co 16e	Tabonuco	vx	0	54	63	7	64	5	5	7	2	17
co 16f	Tabonuco	vx	0	56	78	8	46	5	5	8	2	20
co 16g	Tabonuco	vx	0	44	0	16	11	3	3	0	5	11
co 16h	Tabonuco	vx	0	50	75	7	113	6	6	0	5	16

Field ID	Formation	Rock type	Ni	Ni +/-	Cu	Cu +/-	Zn	Zn +/-	As	As +/-	Rb	Rb +/-	Hg	Hg +/-
co 18a	Tabonuco	mvx	0	58	62	7	114	6	6	0	5	10	0	11
co 19a	Tabonuco	mvx	0	44	228	9	41	4	4	0	5	20	0	9
co 20a	Tabonuco	mvx	0	51	31	6	21	4	4	0	6	44	0	9
co 23a	Tabonuco	vx	52	16	63	6	93	5	5	0	5	17	13	3
co 23b	Tabonuco	vx	0	65	140	9	155	7	7	0	6	12	24	4
co 23c	Tabonuco	vx	0	61	80	8	59	5	5	0	6	34	0	11
co 23d	Tabonuco	vx	3483	49	0	27	38	4	4	0	4	0	0	8
co 23e	Tabonuco	vx	0	49	36	6	41	4	4	0	5	10	0	9
co 23f	Tabonuco	vx	0	47	28	6	54	5	5	0	6	18	12	3
co 17a	Tabonuco	vx	0	61	54	7	55	5	5	0	6	6	0	10
co 17b	Tabonuco	vx	0	60	52	7	39	5	5	8	2	0	0	10
co 18b	Tabonuco	vx	0	64	108	8	68	5	5	8	2	0	0	10
co 23a	Tabonuco	vx	0	74	112	8	234	9	9	0	6	12	14	4
co 23e	Tabonuco	vx	2374	40	0	24	26	4	4	0	4	0	0	8
co 23e_1	Tabonuco	vx	2931	46	40	9	57	5	5	0	4	0	0	9
co 22s	Tabonuco	vx		32	85	5	42	3	3		3	6		5
co 22s	Tabonuco	vx		47	148	8	76	5	5		5	10		8
co 15a	Tabonuco	vx	0	39	0	15	28	4	4	0	4	5	9	3
co 14a	Tabonuco	vx	0	63	153	9	66	6	6	0	6	44	0	11
co 14b	Tabonuco	vx	0	73	35	7	102	7	7	7	2	11	0	12
co 14c	Tabonuco	vx	0	42	94	6	99	4	4	0	4	6	0	7
co 14d	Tabonuco	vx	0	147	67	12	59	9	9	0	16	15	0	15
co 14e	Tabonuco	vx	0	55	54	7	140	7	7	34	3	6	0	10
co 14f	Tabonuco	vx	102	17	139	8	777	15	15	0	5	35	0	9
co 14g	Tabonuco	vx	130	16	177	8	259	7	7	10	2	42	0	8
co 14h	Tabonuco	vx	0	50	0	16	34	4	4	0	5	20	0	10
co 15a	Tabonuco	vx	127	14	70	6	274	7	7	5	1	2	0	7
co 16a	Tabonuco	vx	0	44	47	6	54	4	4	6	1	4	0	8
co 16b	Tabonuco	vx	0	51	0	16	115	6	6	0	5	6	12	3
co 16c	Tabonuco	vx	0	60	35	6	67	5	5	20	2	0	0	11

co 16d	Tabonuco	vx	0	58	0	18	42	5	5	17	2	7	0	11
co 16e	Tabonuco	vx	0	54	63	7	64	5	5	7	2	17	0	10
co 16f	Tabonuco	vx	0	56	78	8	46	5	5	8	2	20	0	10
co 16g	Tabonuco	vx	0	44	0	16	11	3	3	0	5	11	0	9
co 16h	Tabonuco	vx	0	50	75	7	113	6	6	0	5	16	0	9

Field ID	Formation	Rock type	Ti	Ti +/-	Cr	Cr +/-	Mn	Mn +/-	Fe	Fe +/-	Co	Co +/-
co 1a	Unnamed	mvx	726	434		127	33778	313	69695	567	1164	77
co 1b	Unnamed	mvx	196	51		138	31996	319	84843	724	1068	88
co 1c	Unnamed	mvx	14624	527		116	5641	98	103192	840	1464	95
co 1d	Unnamed	mvx	1591	689		200	828	80	265199	2401	2513	171
co 1a	Unnamed	mvx	2757	297	0	99	34379	281	33507	265	1039	50
co 1b	Unnamed	mvx	4581	311		90	7854	96	59439	420	1058	62
co 1c	Unnamed	mvx	8281	337		77	424	30	46578	336	949	55
co 1d	Unnamed	mvx	4111	394		119	3048	74	106162	856	2529	100
co 22a	Unnamed	mvx	448	353	0	92	870	42	35470	324	726	58
co 22b	Unnamed	mvx	368	377	107	35	1016	47	43061	401	844	66
co 22c_1	Unnamed	mvx	3122	368	0	113	3480	79	61836	560	812	78
co 22c_2	Unnamed	mvx	638	493	0	140	6980	122	118260	1058	966	109
co 22c_3	Unnamed	mvx	2999	35	0	107	2986	72	63205	559	966	78
co 22d	Unnamed	mvx	3347	353	0	107	1507	56	59090	534	994	77
co 22f	Unnamed	mvx	3152	344	0	103	3363	75	53478	474	699	70
co 22g	Unnamed	mvx	6118	385	125	36	1570	55	61020	525	1321	76
co 22h	Unnamed	mvx	5168	391	0	107	1161	51	63412	558	1126	79
co 22i	Unnamed	mvx	52	398	126	39	1056	52	63662	580	822	80
co 22j	Unnamed	mvx	4279	384	0	107	2255	66	42030	416	545	67
co 22k	Unnamed	mvx	147	221	0	68	565	29	14003	135	217	32
co 22l	Unnamed	mvx	3894	333	0	92	527	36	47737	389	604	61
co 22m	Unnamed	mvx	577	383	0	102	865	45	58973	497	867	71

co 22n	Unnamed	mvx	4241	327	0	87	1076	44	37866	337	618	58
co 22o	Unnamed	mvx	998	223	0	68	208	23	22229	185	375	39
co 22p	Unnamed	mvx	4448	327	0	87	226	30	38788	323	764	56
co 22q	Unnamed	mvx	385	35	0	83	179	27	27892	253	520	49
co 22a	Unnamed	mvx	4254	354	103	33	1486	50	40195	358	705	61
co 22b	Unnamed	mvx	4222	723	0	241	1918	106	367449	3512	2609	212
co 22c	Unnamed	mvx	2617	359	0	114	3429	78	65355	581	875	79
co 22d	Unnamed	mvx	6451	786	0	263	0	286	451610	4342	1916	233
co 22e	Unnamed	mvx	3753	377	0	104	658	44	42329	423	614	69
co 22p	Unnamed	mvx	3424	367	0	101	547	39	58157	477	624	68

Field ID	**Formation**	**Rock type**	**Ni**	**Ni +/-**	**Cu**	**Cu +/-**	**Zn**	**Zn +/-**	**As**	**As +/-**	**Rb**	**Rb +/-**
co 1a	Unnamed	mvx		55	653	15	164	7	7	2	8	1
co 1b	Unnamed	mvx		60	769	17	186	8		5	3	1
co 1c	Unnamed	mvx		55	170	9	25	4	6	2	6	1
co 1d	Unnamed	mvx		84	324	13	57	6		7	21	1
co 1a	Unnamed	mvx	61	15	541	12	147	6	5	1	9	1
co 1b	Unnamed	mvx		44	275	9	62	4		4		2
co 1c	Unnamed	mvx		41	62	5	20	3		4		2
co 1d	Unnamed	mvx		58	409	12	40	5		6	8	1
co 22a	Unnamed	mvx	0	49	260	10	47	5	0	5	10	1
co 22b	Unnamed	mvx	0	52	233	10	77	6	0	5	4	1
co 22c_1	Unnamed	mvx	0	57	226	10	121	7	0	5	6	1
co 22c_2	Unnamed	mvx	0	66	155	9	216	8	9	2	13	1
co 22c_3	Unnamed	mvx	0	54	492	14	94	6	0	5	7	1
co 22d	Unnamed	mvx	0	56	723	17	67	6	0	6	6	1
co 22f	Unnamed	mvx	0	53	208	10	122	6	7	2	6	1
co 22g	Unnamed	mvx	0	54	31	6	72	5	0	5	4	1
co 22h	Unnamed	mvx	0	54	84	7	50	5	0	5	6	1
co 22i	Unnamed	mvx	0	56	97	8	57	5	0	5	3	1
co 22j	Unnamed	mvx	0	54	109	8	96	6	0	5	0	3
co 22k	Unnamed	mvx	64	14	97	6	90	5	0	4	13	1

co 22l	Unnamed	mvx	0	48	76	6	53	4	0	5	15	1
co 22m	Unnamed	mvx	0	49	65	6	58	5	0	5	28	1
co 22n	Unnamed	mvx	0	47	259	10	38	4	0	5	0	3
co 22o	Unnamed	mvx	0	39	76	6	26	3	0	4	6	1
co 22p	Unnamed	mvx	0	47	60	6	56	4	0	4	23	1
co 22q	Unnamed	mvx	0	43	0	14	42	4	0	5	17	1
co 22a	Unnamed	mvx	0	48	52	6	59	5	5	2	10	1
co 22b	Unnamed	mvx	0	103	604	18	103	8	0	9	21	2
co 22c	Unnamed	mvx	0	55	237	10	121	6	6	2	4	1
co 22d	Unnamed	mvx	0	108	1231	26	24	7	0	10	16	1
co 22e	Unnamed	mvx	0	56	59	7	39	5	0	5	5	1
co 22p	Unnamed	mvx	0	50	450	12	58	5	0	5	24	1

Field ID	Formation	Rock type	Sr	Sr +/-	Zr	Zr +/-	Mo	Mo +/-	Ag	Ag +/-	Ba	Ba +/-	Hg	Hg +/-
co 1a	Unnamed	mvx	6	1	124	2	27	2		25	1360	154		9
co 1b	Unnamed	mvx	11	1	128	2	36	2		26	1138	172		10
co 1c	Unnamed	mvx	5	1	224	3	11	2		26	748	165	10	3
co 1d	Unnamed	mvx	11	1	189	3		7		30	1811	248		11
co 1a	Unnamed	mvx		2	62	2	23	2		22	931	113		8
co 1b	Unnamed	mvx	13	1	77	2	10	2		22	681	110		7
co 1c	Unnamed	mvx		2	105	2		5		22	558	108		7
co 1d	Unnamed	mvx	8	1	89	2	9	2		26	587	144		9
co 22a	Unnamed	mvx	441	5	85	2	0	6	36	9	863	124	0	9
co 22b	Unnamed	mvx	611	7	76	3	0	7	0	28	1209	138	0	10
co 22c_1	Unnamed	mvx	366	5	67	2	7	2	40	9	591	135	17	4
co 22c_2	Unnamed	mvx	177	3	87	2	0	7	36	10	980	176	16	4
co 22c_3	Unnamed	mvx	364	5	68	2	0	6	30	9	0	382	12	4
co 22d	Unnamed	mvx	376	5	52	2	0	7	0	28	0	379	0	10
co 22f	Unnamed	mvx	291	4	68	2	0	6	54	9	488	125	0	10

co 22g	Unnamed	mvx	42	2	74	2	0	6	0	27	0	389	0	9
co 22h	Unnamed	mvx	197	3	61	2	0	6	45	9	607	136	0	10
co 22i	Unnamed	mvx	311	4	61	2	0	7	43	10	502	139	0	9
co 22j	Unnamed	mvx	400	5	64	2	0	7	0	30	602	134	0	11
co 22k	Unnamed	mvx	169	3	36	2	11	2	46	8	259	81	9	3
co 22l	Unnamed	mvx	228	3	83	2	7	2	26	8	927	120	0	8
co 22m	Unnamed	mvx	254	4	65	2	0	6	45	9	778	132	0	9
co 22n	Unnamed	mvx	355	5	81	2	0	6	29	9	0	334	13	3
co 22o	Unnamed	mvx	57	1	30	1	26	2	46	8	501	85	0	7
co 22p	Unnamed	mvx	344	4	77	2	0	6	49	8	777	114	0	9
co 22q	Unnamed	mvx	243	3	78	2	0	6	32	9	720	109	0	9
co 22a	Unnamed	mvx	398	5	83	2	0	6	0	27	870	125	14	3
co 22b	Unnamed	mvx	185	4	60	2	0	7	52	11	1675	282	0	15
co 22c	Unnamed	mvx	331	5	65	2	0	6	42	9	598	134	0	10
co 22d	Unnamed	mvx	27	2	8	2	8	2	0	33	916	300	0	13
co 22e	Unnamed	mvx	207	4	60	2	0	7	40	10	549	133	0	10
co 22p	Unnamed	mvx	358	4	80	2	0	6	0	25	1600	138	0	9